

Distribution and generation of quantum coherence for Gaussian states in de Sitter space

Qianqian Liu¹, Cuihong Wen^{1 *}, Jieci Wang^{1†}, Jiliang Jing^{1‡}

¹ *Department of Physics, and Synergetic Innovation Center for Quantum Effects and Applications, Hunan Normal University, Changsha, Hunan 410081, China*

Abstract

We study the distribution and generation of quantum coherence for two-mode and multi-mode Gaussian states in de Sitter space. It is found that the quantum coherence is redistributed among the mode in different open charts under the curvature effect of de Sitter space. In particular, the Gaussian coherence for the initially correlated state is found to survive in the limit of infinite curvature, while quantum entanglement vanishing in this limit. Unlike entanglement and steering, the coherence of a massive scalar field is more robust than a massless field under the influence of curvature of de Sitter space. In addition, it is shown that the curvature generates two-mode Gaussian state and three-mode Gaussian state quantum coherence among the open charts, even though the observers are localized in causally disconnected regions. It is worth noting that the gravity-generated three-mode coherence is extremely sensitive to the curvature effect for the conformal and massless scalar fields, which may be in principle employed to design an effective detector for the space curvature.

* Email: cuihong_wen@hunnu.edu.cn

† Email: jcwang@hunnu.edu.cn

‡ Email: jljing@hunnu.edu.cn

I. INTRODUCTION

The Quantum state superposition principle is one of the most fundamental features of quantum theory, which distinguishes classical theory. As a key aspect of quantum physics, quantum coherence is an embodiment of the superposition principle of states and is the basis of phenomena such as quantum entanglement and multi-particle interference [1–3]. With the help of quantum coherence, one can implement various quantum information processing tasks that cannot be accomplished classically, such as quantum computing [4, 5], quantum metrology [6, 7], quantum biology [8, 9], and other quantum information storage [10] and transmission [11, 12] tasks. Despite the fundamental importance of quantum coherence, the quantum resource study of coherence receives increasing attention until Baumgratz *et. al.* introduced the framework for the measurement of coherence [1]. Motivated by this, more and more measurements of coherence have been performed [13–17] in recent years. Recently, Xu proposed a quantification of coherence for continuous-variable quantum systems [18], which performs the framework of a quantum resource theory for infinite-dimensional quantum states in quantum optics [19].

Understanding quantum effects in the framework of relativity [20–35] is essential. For example, it was found that nonclassical correlations are generated between the open charts in the exponentially expanding de Sitter space [36–42]. Interestingly, the entanglement remains nonzero even if the distance between the two regions becomes larger than the Hubble length. This means there exists a nonclassical correlation between two causally disconnected regions and the existence of the entanglement means that the Reeh-Schlieder theorem [43] holds in de Sitter space. People cannot understand this phenomenon without the combination of quantum information theory and relativity. In addition, the quantum discord [44] and quantum steering [45] of field modes are also found to be generated between two disconnected open charts under the influence of the space curvature of de Sitter space.

In this paper, we study the distribution and generation of continuous-variable quantum coherence in the background of de Sitter space. The considered initial state is a two-mode squeezed Gaussian state, which can be employed to define particle states when the space-time has at least two asymptotically flat regions [21, 24, 26, 27, 42]. It has a special role in quantum field theory because the field modes in causally disconnected regions are found to be pair-wise squeezed under the influence of spacetime structure evolution and relativistic effects [20–22, 42, 45]. In addition, as the most typical entangled state for continuous variables, the two-mode squeezed state can be

produced with existing technology and be exploited for a few important continuous-variable quantum information tasks [46]. It is found that two-mode and three-mode quantum coherence are generated among the open charts, even though the observers are causally disconnected.

The organization of the paper is as follows. In Sec. II we review the dynamics of field modes in de Sitter space and through the Bogoliubov transformations, the Bunch-Davies vacuum can be represented by the open charts vacuum of the de Sitter space. In Sec. III we discuss the method of measuring the quantum coherence of continuous variables. In Sec. IV we study the behavior of quantum coherence between the two-mode and three-mode Gaussian states in de Sitter space. In the final section, we summarize our results.

II. QUANTIZATION OF SCALAR FIELD IN DE SITTER SPACE

In this section, we review the method developed by Maldacena and Pimentel to obtain the quantization of the scalar field in de Sitter space [36, 38] with some comments on the parameters that relevant to the discussion of quantum coherence. The four-dimensional Euclidean de Sitter space can be embedded in the Five-dimensional Euclidean space. Therefore, the coordinate frames of open charts in de Sitter space can be obtained by analytic continuation from the Euclidean metric [37] respectively,

$$\begin{aligned} ds_R^2 &= H^{-2} \left[-dt_R^2 + \sinh^2 t_R (dr_R^2 + \sinh^2 r_R d\Omega^2) \right], \\ ds_L^2 &= H^{-2} \left[-dt_L^2 + \sinh^2 t_L (dr_L^2 + \sinh^2 r_L d\Omega^2) \right], \end{aligned} \quad (1)$$

where H^{-1} is the Hubble radius and $d\Omega^2$ is the metric on the two-sphere.

The solutions of the Klein-Gordon equation in de Sitter space are found to be $u_{\sigma plm}(t, r, \Omega) \sim \frac{H}{\sinh t_{R(L)}} \chi_{p,\sigma}(t_{R(L)}) Y_{p\ell m}(r_{R(L)}, \Omega)$, where $Y_{p\ell m}$ is a harmonic function on the three-dimensional hyperbolic space. The positive frequency mode functions $\chi_{p,\sigma}(t_{R(L)})$ corresponding to Euclidean vacuum(the Bunch-Davies vacuum), which are supported in both R and L regions derived by Sasaki, Tanaka and Yamamoto in [36]. The index $\sigma = \pm 1$ distinguishing the independent solutions for each open charts and the parameter p is regarded as the curvature parameter of de Sitter space because the effect of curvature appears around $p \sim 1$ and increases through p less than 1. In addition, the limit of infinite curvature appears at $p \rightarrow 0$ [42, 44]. The normalization coefficient for function $\chi_{p,\sigma}(t_{R(L)})$ is $N_p = \frac{4 \sinh \pi p \sqrt{\cosh \pi p - \sigma \sin \pi \nu}}{\sqrt{\pi} |\Gamma(\nu + ip + \frac{1}{2})|}$. The mass parameter ν is defined by $\nu = \sqrt{\frac{9}{4} - \frac{m^2}{H^2}}$, which has two special values: $\nu = 1/2$ for the conformally coupled scalar field,

and $\nu = 3/2$ for the minimally coupled massless scalar field.

With these positive frequency mode functions, the scalar field can be expanded in terms of the creation and annihilation operators

$$\hat{\phi}(t, r, \Omega) = \frac{H}{\sinh t} \int dp \sum_{\sigma, \ell, m} \left[a_{\sigma p \ell m} \chi_{p, \sigma}(t) + a_{\sigma p \ell - m}^\dagger \chi_{p, \sigma}^*(t) \right] Y_{p \ell m}(r, \Omega), \quad (2)$$

where $a_{\sigma p \ell m} |0\rangle_{\text{BD}} = 0$ and the commutation relations are $[a_{\sigma p \ell m}, a_{\sigma' p' \ell' m'}^\dagger] = \delta(p - p') \times \delta_{\sigma, \sigma'} \delta_{l, l'} \delta_{m, m'}$. In the following the indices p, l, m of the operators and mode functions are omitted for simplicity.

By introducing the creation and annihilation operators in different open charts, one can calculate the Bogoliubov transformations [36, 38] between the operators which are defined in the Bunch-Davies vacuum and the open charts vacua, respectively. Then the Bunch-Davies vacuum is found to be [36, 38]

$$|0\rangle_{\text{BD}} = \sqrt{1 - |\gamma_p|^2} \sum_{n=0}^{\infty} (\gamma_p)^n |n\rangle_{\text{L}} |n\rangle_{\text{R}}, \quad (3)$$

where we defined $|n; plm\rangle = \frac{1}{\sqrt{n!}} (c_R^\dagger)^n |0\rangle_{R'}$, and $|\gamma_p| < 1$ should be satisfied. In Eq. (3), the parameter γ_p is

$$\gamma_p = i \frac{\sqrt{2}}{\sqrt{\cosh 2\pi p + \cos 2\pi\nu} + \sqrt{\cosh 2\pi p + \cos 2\pi\nu + 2}}. \quad (4)$$

For the conformally coupled scalar field ($\nu = 1/2$) and the minimally coupled massless scalar field ($\nu = 3/2$), it simplifies to $|\gamma_p| = e^{-\pi p}$.

III. MEASUREMENT OF QUANTUM COHERENCE FOR CONTINUOUS VARIABLES

For a two-mode continuous variable quantum system, we define the vector of field quadratures (position and momentum) operators as $\hat{R} = (\hat{x}_A, \hat{p}_A, \hat{x}_B, \hat{p}_B)$, which are related to the annihilation \hat{a}_i and creation \hat{a}_i^\dagger operators of each mode, by the relations $\hat{x}_i = \frac{(\hat{a}_i + \hat{a}_i^\dagger)}{\sqrt{2}}$ and $\hat{p}_i = \frac{(\hat{a}_i - \hat{a}_i^\dagger)}{\sqrt{2}i}$. The vector operator satisfies the commutation relationship: $[\hat{R}_i, \hat{R}_j] = i\Omega_{ij}$, with $\Omega = \bigoplus_1^{n+m} \begin{pmatrix} 0 & 1 \\ -1 & 0 \end{pmatrix}$ being symplectic form. The first and second moments of a two-mode Gaussian state ρ_{AB} can completely describe all its properties. For the bipartite state ρ_{AB} , its covariance matrix has the form

$$\sigma \equiv \begin{pmatrix} \alpha & \gamma \\ \gamma^T & \beta \end{pmatrix}, \quad (5)$$

where $\alpha = \text{dig}(a, a)$, $\beta = \text{dig}(b, b)$, and $\gamma = \text{dig}(c_+, c_-)$ are 2×2 real matrices. The symplectic eigenvalues of the two-mode Gaussian covariance matrix Eq. (5) are $2\nu_{\mp}^2 = \Delta \mp \sqrt{\Delta^2 - 4I_4}$ with $\Delta = a^2 + b^2 + 2c_+c_-$, $I_4 = \det(\sigma)$.

As shown in [18], the continuous variable quantum coherence of a m -mode Gaussian states can be measured by $C(\rho) = \inf S(\rho||\delta)$, where $S(\rho||\delta) = \text{tr}(\rho \log_2 \rho) - \text{tr}(\rho \log_2 \delta)$ is the relative entropy, δ is an incoherent Gaussian state and \inf runs over all incoherent Gaussian states. In addition, The entropy of ρ is defined by [47]

$$S(\rho) = -\text{tr}(\rho \log_2 \rho) = \sum_{i=1}^m f(\nu_i), \quad (6)$$

where $f(\nu_i) = \frac{\nu_i+1}{2} \log_2 \frac{\nu_i+1}{2} - \frac{\nu_i-1}{2} \log_2 \frac{\nu_i-1}{2}$, and ν_i is symplectic eigenvalues of each mode. Then one obtains the definition of the quantum coherence of Gaussian states [18]

$$C(\rho) = -S(\rho) + \sum_{i=1}^m [(\bar{n}_i + 1) \log_2(\bar{n}_i + 1) - \bar{n}_i \log_2 \bar{n}_i], \quad (7)$$

where $\bar{n}_i = \frac{1}{4}(\sigma_{11}^i + \sigma_{22}^i + [d_1^i]^2 + [d_2^i]^2 - 2)$ is the mean occupation value. Here, σ^i are elements of the subsystem of mode i in a continuous variable matrix, respectively, and $[d^i]^2$ is i first statistical moment of the k mode.

IV. DISTRIBUTION OF GAUSSIAN QUANTUM COHERENCE IN DE SITTER SPACE

A. Reduction of quantum coherence between initially correlated modes

In the subsection, we study the Gaussian quantum coherence between the global observer Alice and the open chart observer Bob (in region R). We use the form of the covariance matrix to describe the initial state ρ_{AB} prepared by the two-mode squeezed Gaussian state in Bunch-Davies vacuum

$$\sigma_{AB}^{(G)}(s) = \begin{pmatrix} \cosh(2s)I_1 & \sinh(2s)Z_1 \\ \sinh(2s)Z_1 & \cosh(2s)I_1 \end{pmatrix}, \quad (8)$$

where s is the squeezing of the initial state and $I_1 = \begin{pmatrix} 1 & 0 \\ 0 & 1 \end{pmatrix}$, $Z_1 = \begin{pmatrix} 1 & 0 \\ 0 & -1 \end{pmatrix}$.

From Eq. (3), we can see the Bunch-Davies vacuum for a global observer can be expressed as a two-mode squeezed state of the R and L vacua [36–38, 42, 44]. In the phase space, The two-mode

squeezing transformation can be expressed by a symplectic operator [42]

$$S_{B,\bar{B}}(\gamma_p) = \frac{1}{\sqrt{1-|\gamma_p|^2}} \begin{pmatrix} I_1 & |\gamma_p|Z_1 \\ |\gamma_p|Z_1 & I_1 \end{pmatrix}. \quad (9)$$

Under this symplectic matrix transformation, the virtual observer anti-Bob is mapped from Bob in the chart R to chart L . Then we can calculate the covariance matrix $\sigma_{AB\bar{B}}$ of the entire state, which is

$$\begin{aligned} \sigma_{AB\bar{B}}(s, \gamma_p) &= [I_A \oplus S_{B,\bar{B}}(\gamma_p)] [\sigma_{AB}^{(G)}(s) \oplus I_{\bar{B}}] \\ &\quad [I_A \oplus S_{B,\bar{B}}(\gamma_p)] \\ &= \begin{pmatrix} \sigma_A & \mathcal{E}_{AB} & \mathcal{E}_{A\bar{B}} \\ \mathcal{E}_{AB}^\top & \sigma_B & \mathcal{E}_{B\bar{B}} \\ \mathcal{E}_{A\bar{B}}^\top & \mathcal{E}_{B\bar{B}}^\top & \sigma_{\bar{B}} \end{pmatrix}, \end{aligned} \quad (10)$$

where $\sigma_{AB}^{(G)}(s) \oplus I_{\bar{B}}$ is the initial covariance matrix for the entire system. In the above expression the diagonal elements are:

$$\sigma_A = \cosh(2s)I_1, \quad (11)$$

$$\sigma_B = \frac{|\gamma_p|^2 + \cosh(2s)}{1 - |\gamma_p|^2} I_1, \quad (12)$$

and

$$\sigma_{\bar{B}} = \frac{1 + |\gamma_p|^2 \cosh(2s)}{1 - |\gamma_p|^2} I_1, \quad (13)$$

Similarly, the non-diagonal elements are found to be $\mathcal{E}_{AB} = \frac{\sinh(2s)}{\sqrt{1-|\gamma_p|^2}} Z_1$, $\mathcal{E}_{B\bar{B}} = \frac{|\gamma_p|(\cosh(2s)+1)}{1-|\gamma_p|^2} Z_1$, and $\mathcal{E}_{A\bar{B}} = \frac{|\gamma_p| \sinh(2s)}{\sqrt{1-|\gamma_p|^2}} I_1$.

Because the charts R and L are causally disconnected in de Sitter space, Bob can not approach the mode \bar{B} on the other side of the event horizon. Therefore, we obtain the covariance matrix $\sigma_{AB}(s, \gamma_p)$ for Alice and Bob by tracing over the mode \bar{B}

$$\sigma_{AB}(s, \gamma_p) = \begin{pmatrix} \cosh(2s)I_1 & \frac{\sinh(2s)}{\sqrt{1-|\gamma_p|^2}} Z_1 \\ \frac{\sinh(2s)}{\sqrt{1-|\gamma_p|^2}} Z_1 & \frac{|\gamma_p|^2 + \cosh(2s)}{1-|\gamma_p|^2} I_1 \end{pmatrix}. \quad (14)$$

We know that the symplectic matrix σ_{AB} is a case of the smallest mixed Gaussian state according to the eigenvalues of the partially transposed symplectic matrix. For Eq. (14), we obtain $\Delta^{(AB)} = 1 + \frac{(1+|\gamma_p|^2 \cosh(2s))^2}{(1-|\gamma_p|^2)^2}$, and $I_4^{AB} = \frac{(1+|\gamma_p|^2 \cosh(2s))^2}{(1-|\gamma_p|^2)^2}$. This mean occupation numbers operator

for each mode from the covariance matrix is

$$\begin{aligned}\bar{n}_A &= \frac{1}{2}(\cosh(2s) - 1), \\ \bar{n}_B &= \frac{1}{2}\left(\frac{|\gamma_p|^2 + \cosh(2s)}{1 - |\gamma_p|^2} - 1\right),\end{aligned}\tag{15}$$

The quantum coherence of this state can be calculated via Eq. (7).

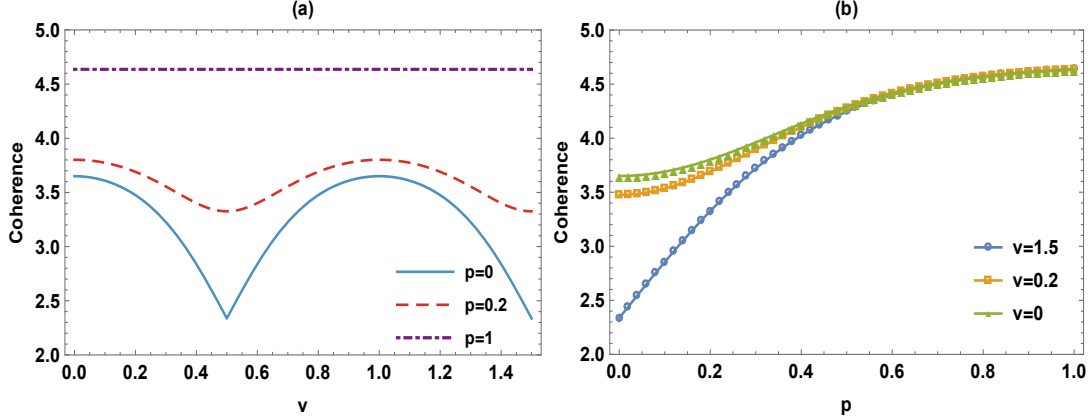


FIG. 1: (Color online). (a) Plots of the quantum coherence as a function of the mass parameter ν , where $p = 1$ (purple dotted line), $p = 0$ (blue solid line), $p = 0.2$ (red dotted line). (b) The Gaussian quantum coherence between Alice and Bob as a function of the curvature parameter p . The green triangle line is for $\nu = 0$, the orange rectangular line is for $\nu = 1/5$ and the blue circular line is for $\nu = 3/2$. Fix the initial state squeezing parameter $s = 1$.

In Fig. 1(a) and Fig. 1(b), we plot the accessible quantum coherence between Alice and Bob as functions of the curvature parameter p and mass parameter ν for a fixed initial squeezing parameter $s = 1$. Fig. 1(a) illustrates that the Gaussian quantum coherence is not influenced by the mass parameter ν in the flat space limit $p = 1$. For any $p \neq 1$, the degree of quantum coherence is a periodic function of the mass parameter ν with period 1. In the infinite curvature limit $p = 0$, the Gaussian quantum coherence reaches *non-zero* minimum values for $\nu = 1/2$ (conformal scalar limit) and $\nu = 3/2$ (massless scalar limit). It is a worthing note that the behavior of quantum coherence for the Gaussian state is very different than that of entanglement because the Gaussian entanglement for the state ρ_{AB} directly reduces to zero in the infinite curvature limit [42]. We can see that the quantum entanglement between Alice and Bob disappears at the infinite curvature limit, but the quantum coherence between them still survives. In this limit, the subsystem Bob is fully entangled with antiBob. As a result of the monogamy of quantum entanglement, there is no

entanglement between Alice and Bob. While the quantum coherence still exist because only a in the single-mode structure is required for coherence.

From Fig. 1(b), we can see that the coherence is a monotone-increasing function of p , which means that the effect of space curvature can reduce the quantum coherence of the initial state. It is interesting to note that the massive field ($\nu = 0$ and $\nu = 0.2$) preserve more quantum coherence than the massless scalar field $\nu = 3/2$. That is to say, the coherence of a massive scalar field is more robust than a massless field in de Sitter space. Such behavior did not appear for the quantum entanglement [37, 42] and steering [45] in the de Sitter space.

B. Generating quantum coherence between initially uncorrelated modes

Tracing over the mode B on Eq. (10), we obtain the covariance matrix $\sigma_{A\bar{B}}$

$$\sigma_{A\bar{B}}(s, \gamma_p) = \begin{pmatrix} \cosh(2s) I_1 & \frac{|\gamma_p| \sinh(2s)}{\sqrt{1-|\gamma_p|^2}} I_1 \\ \frac{|\gamma_p| \sinh(2s)}{\sqrt{1-|\gamma_p|^2}} I_1 & \frac{1+|\gamma_p|^2 \cosh(2s)}{1-|\gamma_p|^2} I_1 \end{pmatrix}, \quad (16)$$

The corresponding symplectic value of the covariance matrix $\sigma_{A\bar{B}}$ is found to be $\nu_+ = \frac{|\gamma_p|^2 + \cosh(2s)}{1-|\gamma_p|^2}$ and $\nu_- = 1$. with $\Delta^{(A\bar{B})} = 1 + \frac{(|\gamma_p|^2 + \cosh(2s))^2}{(1-|\gamma_p|^2)^2}$, and $I_4^{A\bar{B}} = \frac{(|\gamma_p|^2 + \cosh(2s))^2}{(1-|\gamma_p|^2)^2}$.

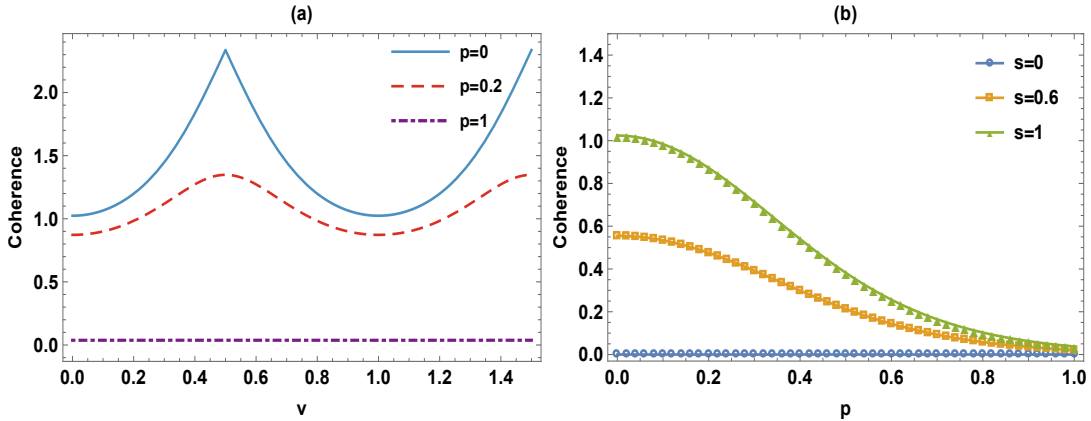


FIG. 2: (Color online). (a) The Gaussian quantum coherence between Alice and anti-Bob as a function of mass parameters ν for different p . The squeezing parameter is fixed as $s = 1$. (b) The quantum coherence as a function of the space curvature parameter p , for different squeezing parameter $s = 1$ (green triangle line), $s = 0.6$ (orange rectangular line), $s = 0$ (blue circular line). The mass parameter is fixed as $\nu = 1$.

Fig. 2(a) shows the quantum coherence between Alice and anti-Bob concerning the mass parameters ν for a fixed initial squeezing parameter $s = 1$. It shows that the Gaussian coherence is

a periodic function versus the mass parameter ν when the space is curved ($p \neq 1$). Like the entanglement in de Sitter space, the quantum coherence of Gaussian state $\rho_{A\bar{B}}$ increases as the effect of space curvature increases. The Fig. 2(b) shows that the coherence is a monotone-decreasing function of p , which means the effect of space curvature can generate quantum coherence between Alice and anti-Bob. Besides, we can see that the larger initial state squeezing parameter, the higher Gaussian quantum coherence between Alice and anti-Bob. In the limit of flat space $p = 1$, regardless of the squeezing parameter and the mass parameter, the quantum coherence about Gaussian state $\rho_{A\bar{B}}$ is zero.

It is worth noting that the bipartite coherence of Alice and anti-Bob is generated by the space curvature in de Sitter space, while the very same curvature also degrades the Alice-Bob coherence. We can understand this from a quantum information theory perspective. We know that quantum coherence can be generated by two-mode squeezed transformation. From Eq. (3), we can see the Bunch-Davies vacuum for a global observer can be expressed as a two-mode squeezed state of the R and L vacua [36–38, 42, 44]. In addition, the virtual observer anti-Bob is mapped from Bob in the chart R to chart L . In other words, the curvature of the de Sitter space is in fact a two-mode squeezed transformation acts on the field modes, as has been shown in Eq. (10). Therefore, the bipartite coherence of Alice-anti-Bob is generated by the two-mode squeezed transformation induced by the space curvature of the de Sitter space, while the degradation of the Alice-Bob coherence because the initial coherence is shared among the entire tripartite system $\sigma_{AB\bar{B}}$.

We know that the modes \bar{B} and B are causally disconnected because the L and R open charts are separated by the event horizon. By tracing off the mode A , we get the covariance matrix between the observer Bob in the R region and the other observer anti-Bob in the L region, which is

$$\sigma_{B\bar{B}}(s, \gamma_p) = \begin{pmatrix} \frac{|\gamma_p|^2 + \cosh(2s)}{1 - |\gamma_p|^2} I_1 & \frac{|\gamma_p|(\cosh(2s) + 1)}{1 - |\gamma_p|^2} Z_1 \\ \frac{|\gamma_p|(\cosh(2s) + 1)}{1 - |\gamma_p|^2} Z_1 & \frac{1 + |\gamma_p|^2 \cosh(2s)}{1 - |\gamma_p|^2} I_1 \end{pmatrix}, \quad (17)$$

from which we obtain the mean occupation numbers is $\bar{n}_B = \frac{1}{2} \left(\frac{|\gamma_p|^2 + \cosh(2s)}{1 - |\gamma_p|^2} - 1 \right)$ and $\bar{n}_{\bar{B}} = \frac{1}{2} \left(\frac{1 + |\gamma_p|^2 \cosh(2s)}{1 - |\gamma_p|^2} - 1 \right)$ of continuous variable matrix $\sigma_{B\bar{B}}$ and calculate the symplectic matrix eigenvalues and the quantum coherence.

In Fig. 3(a), it shows that the quantum coherence between modes B and \bar{B} increases slowly as the enhancement of the effect of space curvature when $\nu = 0$ and $\nu = 0.2$. However, for the conformally coupled scalar field $\nu = 1/2$ and the minimally coupled massless scalar field

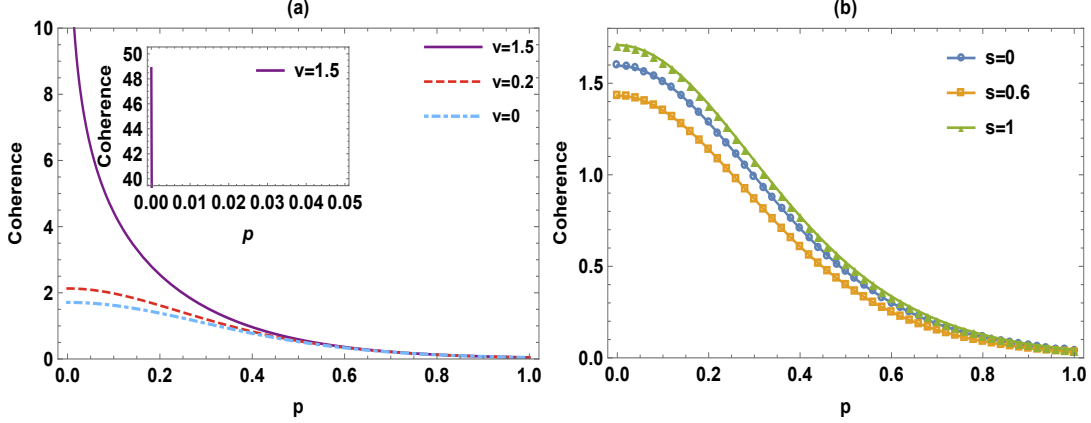


FIG. 3: (color online). (a) The Gaussian quantum coherence between Bob and anti-Bob as a function of the parameter p . Fix the squeezing parameter $s = 1$, and the blue dotted line is for $\nu = 0$, the red dotted line is for $\nu = 1/5$, the purple line is for $\nu = 3/2$. (b) The quantum coherence as a function of the curvature parameter p for different squeezing parameters $s = 0$ (blue circular line), $s = 1$ (green triangle line), $s = 0.6$ (orange rectangular line). Fix the mass parameter $\nu = 1$.

$\nu = 3/2$, the quantum coherence for state $\rho_{B\bar{B}}$ sharply increases and approaches to the maximum when $p \rightarrow 0$. That is to say, the $\rho_{B\bar{B}}$ Gaussian coherence is in fact a sensitive indicator for the space curvature when it in two special cases: the conformally coupled scalar field and the minimally coupled massless scalar field.

Fig. 3(b) also shows that the coherence is a monotone-decreasing function of p . This verifies that the space curvature in de Sitter space generates the Gaussian coherence between the initially uncorrelated observers. Interestingly, unlike the generated Gaussian coherence between modes A and \bar{B} , the quantum coherence between modes B and \bar{B} can be very strong even the squeezing parameter is zero. The generation of Gaussian quantum coherence between the causally disconnected regions of de Sitter space is nontrivial because one can never communicate classically if the observers are separated by the event horizon.

C. Generating quantum coherence between three mode

The quantum coherence among the global observer Alice and two open chart observers Bob and anti-Bob can be obtained through the covariance matrix in Eq. (10). Note that $\det(\sigma_{AB\bar{B}}) = 1$, which means the three-mode Gaussian state is pure, and the symplectic eigenvalues of this state are equal to 1. Thus the quantum coherence of the three-mode Gaussian state can be calculated by

[18]

$$C(\sigma_{AB\bar{B}}) = \sum_{i=1}^3 (\bar{n}_i + 1) \log_2(\bar{n}_i + 1) - \bar{n}_i \log_2 \bar{n}_i, \quad (18)$$

where $\bar{n}_1 = \bar{n}_A$, $\bar{n}_2 = \bar{n}_B$, $\bar{n}_3 = \bar{n}_{\bar{B}}$, whose values obtained from the covariance matrix of the three-mode Gaussian state.

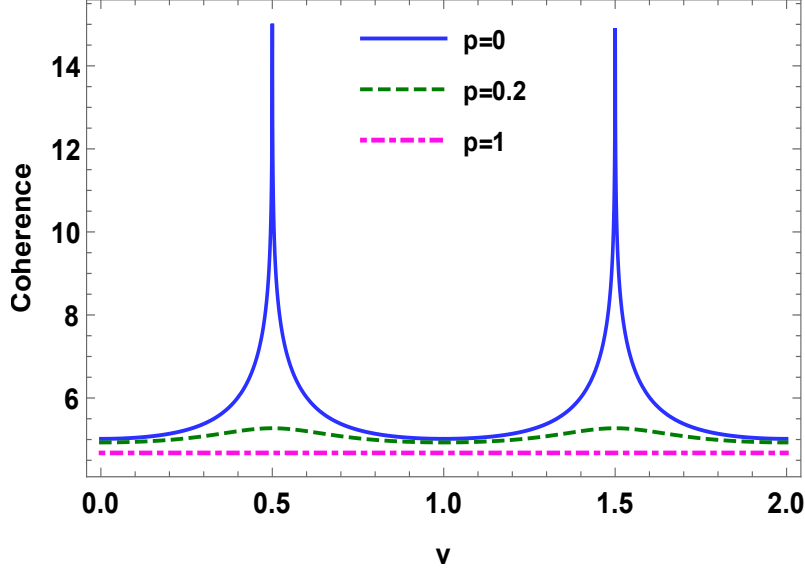


FIG. 4: (color online). The three modes Gaussian quantum coherence between Alice, Bob, and anti-Bob as functions of ν for different p , the squeezing parameter is fixed as $s = 1$.

In Fig. 4, unlike the quantum coherence between mode B and mode \bar{B} , the tripartite quantum coherence does not vanished in the flat space limit $p = 1$. Besides, the tripartite Gaussian quantum coherence slowly changes as a function of ν for $p = 0.2$. However, the generated three-mode quantum coherence is extremely sensitive to the mass parameter ν for $p = 0$, which is very different than the generated quantum coherence for Gaussian state $\rho_{A\bar{B}}$. That is to say, the generated three-mode Gaussian coherence is a much more sensitive indicator of space curvature in the cases of the conformally coupled scalar field and the minimally coupled massless scalar field. This important character can be in principle employed to design an effective detector for the space curvature.

V. CONCLUSIONS

In this work, we study the distribution and generation of quantum coherence for Gaussian states in de Sitter space. It is found that the curvature of the de Sitter space and mass parameter of the field have evident effects on the degree of coherence for all the bipartite and tripartite states. The quantum coherence between mode A and the mode B decreases as the curvature effect in de Sitter space increases. However, it reaches a *non-zero* minimum value in the infinite curvature limit, which is different from that of entanglement in de Sitter space. The massive field is found to preserve more quantum coherence than the massless scalar field for the Gaussian state ρ_{AB} , which did not appear for the quantum entanglement and steering. It is found that the quantum coherence is not only be distributed among the uncorrelated modes in the open-charts but also generates under the curvature effect of de Sitter space. It shows that the quantum coherence between two causally disconnected open-charts can be very strong even if the initial state squeezing parameter is zero, which verifies the space curvature generates Gaussian quantum coherence. Unlike the generated Gaussian state $\rho_{A\bar{B}}$ coherence, the generated three-mode and two-mode $\rho_{B\bar{B}}$ Gaussian coherence are extremely sensitive to curvature effects for conformal and massless scalar fields, which can be employed to design an effective detector for the space curvature.

Acknowledgments

This work is supported by the National Natural Science Foundation of China under Grant No. 11875025; and Science and Technology Planning Project of Hunan Province under Grant No. 2018RS3061; and the Natural Science Fund of Hunan Province under Grant No. 2018JJ1016.

-
- [1] T. Baumgratz, M. Cramer, and M.B. Plenio, *Phys. Rev. Lett.* **2014**, *113*, 140401.
 - [2] A. Streltsov, G. Adesso, and M.B. Plenio, *Rev. Mod. Phys.* **2017**, *89*, 041003.
 - [3] M. Hu, X. Hu, J. Wang, Y. Peng, Y. Zhang, and H. Fan, *Phys. Rep.* **2018**, *762*, 1-100.
 - [4] P.W. Shor, *SIAM J. Comput.* **1997**, *26*, 1484.
 - [5] L.K. Grover, *Phys. Rev. Lett.* **1997**, *79*, 325.
 - [6] V. Giovannetti, S. Lloyd, and L. Maccone, *Science* **2004**, *306*, 1330.
 - [7] V. Giovannetti, S. Lloyd, and L. Maccone, *Nat. Photonics* **2011**, *5*, 222.

- [8] M. B. Plenio, and S. F. Huelga, *New J. Phys.* **2008**, *10*, 113019.
- [9] M. J. Tao, M. Hua, N. N. Zhang, W. T. He, Q. Ai, and F. G. Deng, *Quantum Engineering* **2020**, *2*, e53.
- [10] M. Gndoan, P.M. Ledingham, A. Almasi, M. Cristiani, and H. Riedmatten, *Phys. Rev. Lett.* **2012**, *108*, 190504.
- [11] Y. F. Hsiao, P. J. Tsai, H. S. Chen, S. X. Lin, C. C. Hung, and C. H. Lee, *Phys. Rev. Lett.* **2018**, *120*, 18360.
- [12] Y. Lu, Y-C. Liu, and Y-S. Li, *Chin. Phys. B* . **2020**, *29*, 060301.
- [13] M. Lostaglio, D. Jennings, and T. Rudolph, *Nat. Commun.* **2015**, *6*, 6383.
- [14] Y. Yao, X. Xiao, and L. Ge, *Phys. Rev. A* **2015**, *92*, 022112.
- [15] L. Zhang, *J. Phys. A: Math. Theor* **2017**, *50*, 155303.
- [16] H. Zhang, B. Chen, and M. Li, *Commun. Theor. Phys.* **2017**, *67*, 166.
- [17] G-L. Long, *Physical Review A* **2001**, *64*, 022307.
- [18] J. Xu, *Phys. Rev. A.* **2016**, *93*, 032111.
- [19] S. L. Braunstein, and P. van Loock, *Rev. Mod. Phys.* **2005**, *77*, 513.
- [20] I. Fuentes-Schuller, and R.B. Mann, *Phys. Rev. Lett.* **2005**, *95*, 120404.
- [21] G. Adesso, I. Fuentes-Schuller, and M. Ericsson, *Phys.Rev.A.* **2007**, *76*, 062112.
- [22] M. Aspachs, G. Adesso, and I. Fuentes-Schuller, *Phys. Rev. Lett* **2010**, *105*, 151301.
- [23] T.G. Downes, I. Fuentes-Schuller, and T.C. Ralph, *Phys. Rev. Lett.* **2011**, *106*, 210502.
- [24] D.J. Hosler, C. van de Bruck, and P. Kok, *Phys. Rev. A* **2012**, *85*, 042312.
- [25] N. Friis, A.R. Lee, K. Truong, C. Sabín, E. Solano, G. Johansson, and I. Fuentes-Schuller, *Phys. Rev. Lett.* **2013**, *110*, 113602.
- [26] J. Doukas, E.G. Brown, A. Dragan, and R.B. Mann, *Phys. Rev. A* **2013**, *87*, 012306.
- [27] D. Su, and T.C. Ralph, *Phys. Rev. D* **2014**, *90*, 084022.
- [28] R. Bousso, A. Shahbazi-Moghaddam, and M. Tomaevi, *Phys. Rev. Lett.* **2019**, *123*, 241301.
- [29] T. Liu, J. Jing, and J. Wang, *Adv. Quantum Technol.* **2018**, *1*, 1800072; J. Wang, T. Liu, J. Jing, and S. Chen, *Adv. Quantum Technol.* **2019**, *2*, 1900003.
- [30] J. Wang, H. Cao, J. Jing J, and H. Fan, *Phys. Rev. D* **2016**, *93*, 125011.
- [31] L. Gyongyosi, and I. Sandor, *Quantum Engineering* **2019**, *1*, e23.
- [32] L. Gyongyosi, *Quantum Engineering* **2020**, *2*, e30.
- [33] D. Wang, W-N. Shi, R. D. Hoehn, F. Ming, W-Y. Sun, S. Kais, and L. Ye, *Ann. Phys.*, **2018**, *530*, 1800080.

- [34] F. Ming, D. Wang, and L. Ye, *Ann. Phys.*, **2019**, 531, 1900014.
- [35] F. Ming, X-K. Song, J. Ling, L. Ye, and D. Wang, *Eur. Phys. J. C*, **2020**, 80, 275.
- [36] M. Sasaki, T. Tanaka, and K. Yamamoto, *Phys. Rev. D* **1995**, 51, 2979-2995.
- [37] A. Albrecht, S. Kanno, and M. Sasaki, *Phys. Rev. D* **2018**, 97, 083520.
- [38] J. Maldacena, and G.L. Pimentel, *JHEP* **2013**, 1302, 038.
- [39] S. Kanno, J. Murugan, J.P. Shock, and J. Soda, *JHEP* **2014**, 1407, 072.
- [40] K.K. Ng, R.B. Mann, and E. Mart $\tilde{\text{A}}$ n-Mart $\tilde{\text{A}}$ nez, *Phys. Rev. D* **2018**, 98, 125005.
- [41] C. Arias, F. Diaz, and P. Sundell, *Class. Quantum Grav.* **2020**, 37, 01500.
- [42] J. Wang, C. Wen, J. Jing, and S. Chen, *Phys. Lett. B* **2020**, 800, 135109.
- [43] A. Matsumura. and Y. Nambu, *Phys. Rev. D* **2018**, 98, 025004.
- [44] S. Kanno, J.P. Shock, and J. Soda, *Phys. Rev. D* **2016**, 94, 125014.
- [45] C. Wen, J. Wang, and J. Jing, *Eur. Phys. J. C* **2020**, 80, 78.
- [46] S. L. Braunstein, and P. van Loock, *Rev. Mod. Phys.* **2005**, 77, 513.
- [47] A. S. Holevo, M. Sohma, and O. Hirota, *Phys. Rev. A* **1999**, 59, 1820.